

See discussions, stats, and author profiles for this publication at: <https://www.researchgate.net/publication/262143186>

# NMR Relaxation Enhancement of Water Protons by Gd-Doped Boron Nitride Nanotubes

ARTICLE in THE JOURNAL OF PHYSICAL CHEMISTRY C · FEBRUARY 2014

Impact Factor: 4.77 · DOI: 10.1021/jp412091t

---

READS

68

6 AUTHORS, INCLUDING:



**Lucia Calucci**

Italian National Research Council

75 PUBLICATIONS 843 CITATIONS

SEE PROFILE



**Virgilio Mattoli**

Istituto Italiano di Tecnologia

156 PUBLICATIONS 1,134 CITATIONS

SEE PROFILE



**Barbara Mazzolai**

Istituto Italiano di Tecnologia

196 PUBLICATIONS 1,584 CITATIONS

SEE PROFILE



**Claudia Forte**

Italian National Research Council

104 PUBLICATIONS 905 CITATIONS

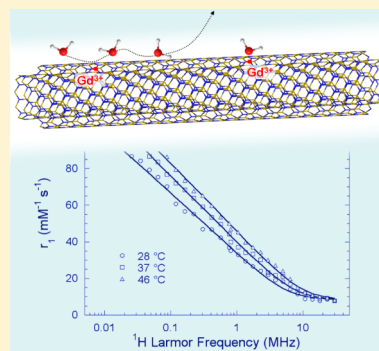
SEE PROFILE

## NMR Relaxation Enhancement of Water Protons by Gd-Doped Boron Nitride Nanotubes

Lucia Calucci,<sup>\*,†</sup> Gianni Ciofani,<sup>‡</sup> Virgilio Mattoli,<sup>‡</sup> Barbara Mazzolai,<sup>‡</sup> Adriano Boni,<sup>§</sup> and Claudia Forte<sup>†</sup><sup>†</sup>Istituto di Chimica dei Composti OrganoMetallici, Consiglio Nazionale delle Ricerche – CNR, Via G. Moruzzi 1, 56124 Pisa, Italy<sup>‡</sup>Center for Micro-BioRobotics @SSSA, Istituto Italiano di Tecnologia, Viale Rinaldo Piaggio 34, 56025 Pontedera (Pisa), Italy<sup>§</sup>Center for Nanotechnology Innovation @NEST, Istituto Italiano di Tecnologia, Piazza San Silvestro 12, 56127 Pisa, Italy

## S Supporting Information

**ABSTRACT:** The longitudinal NMR relaxation rate ( $R_1$ ) of water protons was measured on aqueous suspensions of Gd@BNNTs (i.e., boron nitride nanotubes doped with 0.4% w/w of Gd) coated with glycol-chitosan in the 0.01–30.0 MHz Larmor frequency range, by using a fast field-cycling relaxometer. The dispersion curve of the relaxivity ( $r_1$ ) relative to Gd, determined exploiting  $R_1$  data from Gd@BNNT and BNNT suspensions, shows a logarithmic dependence on frequency which is characteristic of a relaxation enhancement dominated by an outer sphere mechanism governed by two-dimensional diffusion of water in proximity of  $Gd^{3+}$  ions on the BNNT surface. Quantitative information on water diffusion and affinity for the surface was obtained by analyzing the  $r_1$  NMRD curves in terms of a model for two-dimensional diffusion. The effects of the nanotube assembly in water and of the coating hydrophilicity on the interactions between water molecules and  $Gd^{3+}$  ions governing the proton relaxation enhancement at the basis of contrast in magnetic resonance imaging (MRI) are discussed.



## ■ INTRODUCTION

Boron nitride nanotubes (BNNTs) are a relatively new class of nanomaterials showing promising potential in biomedical applications.<sup>1</sup> Indeed, thanks to their special physical and chemical properties,<sup>2–5</sup> they have already been proposed for a number of applications in the field of nanomedicine, from their application as bioimaging trackers to their use as carriers for delivery of chemicals (e.g., drugs, radiochemicals, nucleic acids, proteins, etc.) and/or physical stimuli (e.g., mechanical, electrical, etc.) to living biological entities (cells, tissues, and intact bodies).<sup>6</sup> Very recently, BNNTs doped with  $Gd^{3+}$  (Gd@BNNTs) have been proposed by us as magnetic resonance imaging (MRI) contrast agents (CAs),<sup>7</sup> in analogy to other Gd-doped nanosized systems.<sup>8–19</sup> In fact, at high magnetic field (7 T) Gd@BNNTs were found to display  $T_1$  contrast properties comparable to those of clinically used Gd-based contrast agents, but extremely better  $T_2$  contrast properties,<sup>7</sup> thus holding promise as potential  $T_2$ -weighted MRI contrast agents.

The use of nanostructures to develop novel CAs has been extensively exploited over the past decade,<sup>20,21</sup> their synthetic strategies being based either on covalently and noncovalently functionalizing multiple  $Gd^{3+}$ –chelate complexes onto nanostructures or on encapsulation of  $Gd^{3+}$  ions within the nanostructures. Two main motivations are at the basis of the intensive research in this field. First, the introduction of nanostructures endows other modalities besides MRI, and hence achieves prospects for multimodal probes, in particular allowing simultaneous diagnostic and therapeutic applications. Second, the coupling of a  $Gd^{3+}$  ion with a nanostructure can

affect the water proton paramagnetic relaxation enhancement through its influence on the dynamics of the water molecules. As a matter of fact, nanosized CAs show an increase in longitudinal relaxivity ( $r_1$ , defined as the change in the longitudinal relaxation rate,  $R_1$ , of the water protons per mM concentration of the CA) compared to  $Gd^{3+}$ –chelate complexes widely used in clinical MRI, with the gadonanotubes showing the biggest effect. Moreover, for some nanostructured systems the water proton longitudinal relaxivity dependence on  $^1H$  Larmor frequency, called nuclear magnetic resonance dispersion (NMRD), is considerably different with respect to those of Gd chelates, particularly at low frequencies.<sup>22</sup> Since the NMRD curve provides insight into the interactions between the water molecules and the contrast agent, these findings may be correlated to the presence of multiple relaxation centers and/or to the geometric confinement of water exerted by the nanostructure, which increase the correlation times of the critical dynamic processes, i.e., tumbling of the agent, water exchange into the inner hydration shell, and water diffusion. Finally, changes in shape of the NMRD profile may also arise from an altered dimensionality of the water diffusion.<sup>23</sup> In this context, it has been recognized that the coating used to obtain stable aqueous suspensions of Gd-doped nanostructures may play a role in driving the  $^1H$  relaxation of the surrounding water, by modifying the hydrodynamic size of the particles and

Received: December 10, 2013

Revised: January 29, 2014

Published: February 26, 2014



their aggregation state, and by affecting viscosity and diffusion of water molecules in the proximity of the nanostructure surface, thus regulating the accessibility of water to the paramagnetic centers.

In the present study, an analysis of the NMRD profiles of water protons in aqueous suspensions of Gd@BNNTs is performed to get insight into both the relaxivity properties at low frequency and the mechanism of relaxation enhancement in these systems, with the ultimate goal of understanding the magnetic interactions between water molecules and nanotube assemblies, which are of critical importance for the development of CAs with desired properties.

To this aim Gd@BNNTs were suspended in water using a glycol-chitosan coating, and  $^1\text{H}$  NMRD profiles were acquired at different concentrations and temperatures over the 0.01 to 30 MHz Larmor frequency range using a fast field-cycling (FFC) relaxometer. In order to isolate the contribution of Gd $^{3+}$  paramagnetic centers to the water proton relaxation enhancement,  $^1\text{H}$  NMRD profiles were also acquired on suspensions of glycol-chitosan coated BNNTs and glycol-chitosan alone. The analysis of the data, performed in terms of models for paramagnetic relaxation enhancement (PRE), allowed qualitative and quantitative information to be obtained on the relaxation mechanism dominating water proton relaxivity at different frequencies and, in turn, on water properties in the proximity of the nanotube surface. Such information can be exploited to optimize Gd@BNNT contrast properties.

## EXPERIMENTAL SECTION

**Materials.** The glycol-chitosan-coated BNNT and Gd@BNNT samples were those of a previous work.<sup>7</sup> The Gd content, determined by Inductively Coupled Plasma-Mass Spectrometry (ICP-MS, Agilent Technologies Inc., 7700 series), was  $0.40 \pm 0.01\%$  w/w.<sup>7</sup> Energy dispersive X-ray (EDX) surface analysis revealed the presence of Ti ( $0.21 \pm 0.05\%$  w/w), Ca ( $1.0 \pm 0.1\%$  w/w), and Al ( $0.24 \pm 0.05\%$  w/w), whereas Fe and Cr contents were below the detection limit.<sup>7</sup> In water suspension, Gd@BNNTs had a hydrodynamic radius of about 600 nm, with a polydispersion index of 0.150, and a Z-potential of about 20 mV, as determined by analysis with a Nano Z-Sizer 90 (Malvern Instrument).<sup>7</sup>

In this work, the presence of paramagnetic metal impurities was further checked on both BNNTs and Gd@BNNTs by Inductively Coupled Plasma – Optical Emission Spectroscopy (ICP-OES) analysis using a Varian 720 ES instrument. For the analysis, samples were treated with 65%  $\text{HNO}_3$  and 30%  $\text{H}_2\text{O}_2$  and digested in a Milestone Start D microwave apparatus. For both samples, the analysis revealed a Co content of  $\sim 0.1\%$  w/w and Fe, Cr, and Ni contents under the detection limit (i.e., below  $0.05\%$  w/w).

**Relaxation Time Measurements.** The NMRD profiles for water protons were acquired over the frequency range 0.01–30 MHz with a Spinmaster FFC-2000 NMR relaxometer (Stelar srl, Mede, Italy). The system operated at a measurement frequency of 16.3 MHz for  $^1\text{H}$ , with a  $90^\circ$  pulse duration of 9  $\mu\text{s}$ . The temperature of the samples was controlled within  $\pm 0.5^\circ\text{C}$  with a Stelar VTC90 variable temperature controller.  $T_1$  measurements were performed using the prepolarized (PP) and nonpolarized (NP) pulse sequences<sup>24</sup> below and above 10 MHz, respectively. All of the  $^1\text{H}$  magnetization curves vs time were monoexponential within experimental error and the errors in fitting  $T_1$  were always less than 5%.

## RESULTS AND DISCUSSION

Water proton longitudinal relaxation rates ( $R_1$ ) were measured at  $37^\circ\text{C}$  over the 0.01 to 30 MHz Larmor frequency range on aqueous suspensions of Gd@BNNTs and BNNTs coated with glycol-chitosan (1 mg/mL of nanotubes and glycol-chitosan) and on an aqueous suspension of the sole glycol-chitosan (1 mg/mL); the  $R_1$  dispersions are shown in Figure 1.

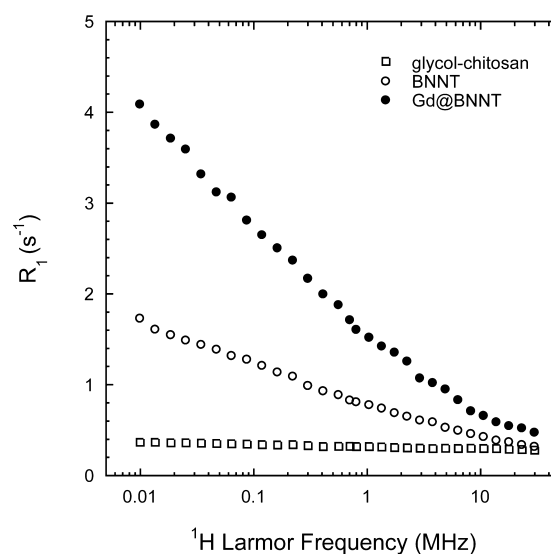


**Figure 1.**  $R_1$  NMRD curves recorded on Gd@BNNT, BNNT, and glycol-chitosan samples (1 mg/mL) at  $37^\circ\text{C}$ .

Both Gd@BNNT and BNNT suspensions show relaxation rates continuously decreasing with increasing the magnetic field, whereas the glycol-chitosan sample is only slightly field dependent. The  $R_1$  dispersion observed for the undoped BNNTs can be ascribed to the presence of residual paramagnetic metal impurities from the synthetic procedure,<sup>25</sup> which, on the basis of our ICP-OES analysis and TEM images reported in ref 25, are most probably cobalt nanoparticles. In Gd@BNNTs the above-mentioned paramagnetic impurities are still present and the additional relaxation enhancement is ascribable to the Gd doping ( $0.4\%$  w/w, as determined in ref 7). The same general behavior of the  $^1\text{H}$  relaxation rate vs Larmor frequency is observed for Gd@BNNT and BNNT suspensions at different concentrations ranging from 0.1 mg/mL to 1 mg/mL, as reported in Figure 2. At each frequency a linear dependence of  $R_1$  on nanotube concentration is found (see Figure S1 in the Supporting Information). These results indicate that there are no concentration-dependent aggregation effects on the interactions of the coated nanotubes with water molecules.

In the fast exchange limit, where the exchange time of water between the bulk and the surface of the coated nanotubes is shorter than the relaxation times in the different environments, the overall water proton relaxation rate,  $R_1$ , is the sum of the relaxation rates in the different environments. Therefore, for water protons in Gd@BNNT suspensions  $R_1$  is given by

$$R_1 = R_1^{\text{bulk}} + R_1^{\text{dia}} + R_1^{\text{BNNT}} + R_1^{\text{Gd}} \quad (1)$$

where  $R_1^{\text{bulk}}$  is the relaxation rate of bulk water protons,  $R_1^{\text{dia}}$  is the relaxation rate of water protons interacting through dipolar interactions and/or chemical exchange with diamagnetic systems present in the sample, that is essentially with the

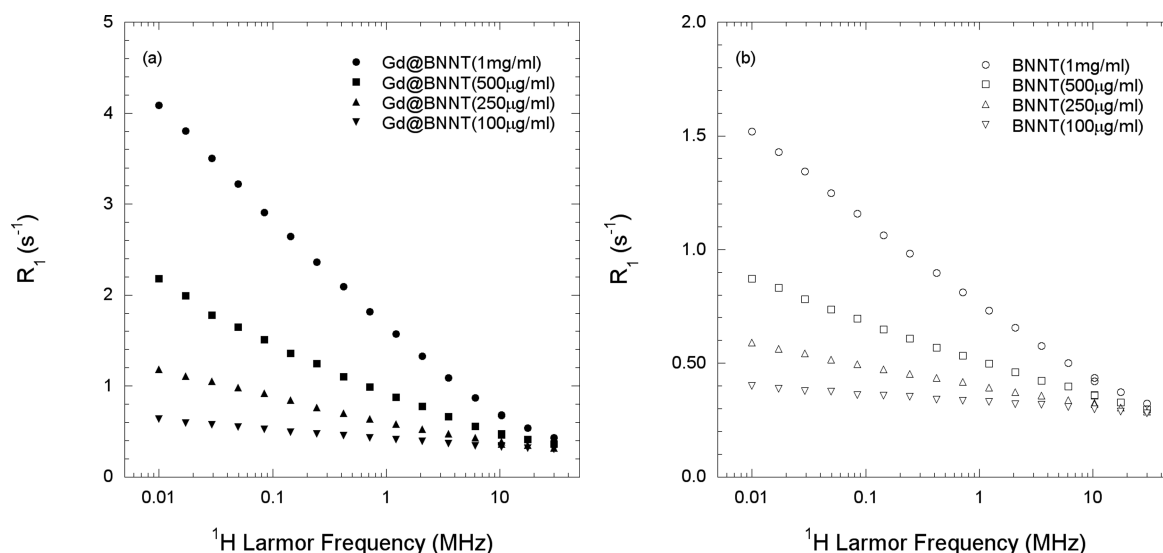


**Figure 2.**  $R_1$  NMRD curves recorded on (a) Gd@BNNT and (b) BNNT samples at different concentrations and 37 °C.

nanotube coating,  $R_1^{\text{BNNT}}$  is the relaxation rate of protons interacting with BNNTs, and  $R_1^{\text{Gd}}$  is the relaxation rate of protons interacting with paramagnetic Gd ions on Gd@BNNT surface. The relaxation term  $R_1^{\text{bulk}}$  has no magnetic field dependence in the studied range because the Larmor frequency is much smaller than the reciprocal of either the rotational or translational correlation time for all accessible magnetic fields; the same can be said for the  $R_1^{\text{dia}}$  contribution on the basis of the  $R_1$  NMRD curves acquired for suspensions of the sole glycol-chitosan (Figure 1). The field dependent contributions can therefore be attributed to paramagnetic relaxation enhancement, the magnetic moment of the paramagnetic species (Co in BNNTs; Co and  $\text{Gd}^{3+}$  ions in Gd@BNNTs) being large. The contribution of gadolinium can be isolated by making the difference between the  $R_1$  values measured at each frequency for Gd@BNNTs and BNNTs, and then used to determine the Gd relaxivity  $r_1$  through eq 2:

$$r_1 = \frac{R_1^{\text{Gd}}}{[\text{Gd}]} \quad (2)$$

where  $[\text{Gd}]$  is the millimolar concentration of  $\text{Gd}^{3+}$  ions. The  $r_1$  NMRD curve obtained for the Gd@BNNTs at 37 °C is shown in Figure 3. A quite high relaxivity is observed at very low fields (0.01 MHz), whereas at the highest magnetic field values corresponding to the standard MRI field strength (20–60 MHz), the relaxivity is  $\sim 9 \text{ s}^{-1} \text{ mM}^{-1}$ . Moreover, in a previous study on the same systems, a relaxivity of  $\sim 3 \text{ s}^{-1} \text{ mM}^{-1}$  was found at 7 T (300 MHz).<sup>7</sup> The relaxivity continuously decreases with increasing the proton Larmor frequency from 0.01 to 10 MHz, and tends to a plateau value between 10 and 30 MHz. The observed NMRD curve is considerably different from those reported so far for  $\text{Gd}^{3+}$  chelates, which present constant values below 1 MHz, a typical high field relaxivity peak centered at 20–40 MHz, and a rapid decrease above these frequencies. The shape of the NMRD curve is also different from those reported for some nanostructured Gd-based CAs, such as gadofullerenes, but quite similar in the low frequency region to those reported for gadonanotubes (i.e., Gd-doped carbon nanotubes),<sup>8,9,16</sup> Gd-ion-doped upconversion nanoparticles,<sup>18</sup> and  $\text{Mn}^{2+}$ -containing graphene nanoplatelets and nanoribbons.<sup>15</sup>

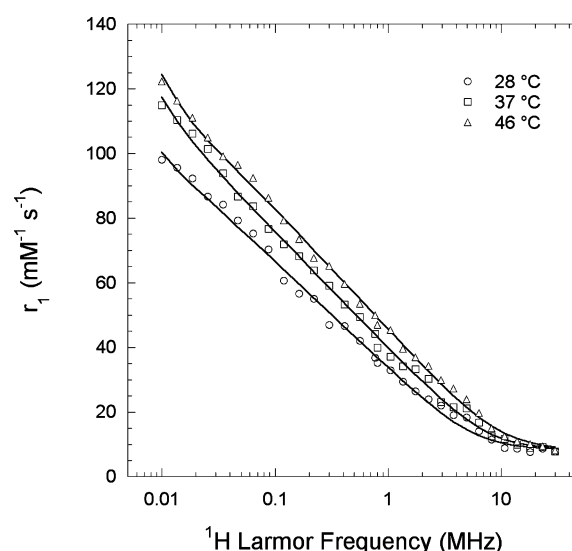


**Figure 3.**  $r_1$  NMRD curves determined for Gd@BNNTs (1 mg/mL) at different temperatures.

Moreover, as shown in Figure 3, the relaxivity  $r_1$  increases with increasing the temperature at Larmor frequencies between 0.01 and 10 MHz and is almost unaffected by the temperature at higher frequencies. A similar behavior has been reported for the longitudinal relaxation rates of water protons in porous media and ascribed to chemical exchange between water molecules interacting with the pore surface and water molecules in the bulk.<sup>26,27</sup>

In order to rationalize the observed NMRD trends, it is necessary to understand the mechanism of relaxation enhancement which may be of relevance in these systems. The paramagnetic relaxation enhancement (PRE) of  $\text{Gd}^{3+}$  ions may originate from either or both the inner sphere (IS) and the outer sphere (OS) mechanisms.<sup>28–31</sup> The IS mechanism involves water molecules residing in the first coordination sphere of  $\text{Gd}^{3+}$  ions, and the associated PRE depends on the number of coordinated water molecules, the mean residence time of water molecules, the rotational correlation time of the object on which the paramagnetic center resides, and the relaxation of the electronic spin associated with the para-



magnetic ion. The OS contribution is due to the movement of the water protons in the proximity of the local magnetic field gradients generated by the paramagnetic ion. In this case, the interaction between proton spins and the magnetic moment is a dipolar interaction modulated by a translational correlation time that takes into account the relative diffusion constant of the paramagnetic center and the water molecule, as well as their distance of closest approach. The overall longitudinal relaxivity is the sum of the IS and OS relaxivities:

$$r_1 = r_1^{\text{IS}} + r_1^{\text{OS}} \quad (3)$$

In our case, the relaxivity dispersion observed for the Gd@BNNT suspensions has a logarithmic dependence on the magnetic field which is characteristic of outer sphere relaxation caused by the diffusive exploration of a two-dimensional space in close proximity to paramagnetic species.<sup>32–37</sup> Indeed, since the Gd<sup>3+</sup> ions are located on the BNNT surface, the diffusion of the water molecules is limited by the excluded volume imposed by the surface, and the time dependence of the re-encounter probability between the water protons and the paramagnetic species is proportional to  $1/t$ . As a consequence, the spectral density function characterizing this motion, which is the Fourier transform of the time correlation function, is logarithmic in the Larmor frequency. The constraint exerted by the nanotubes may effectively create a water layering at the interface, where more frequent re-encounters between diffusing water molecules and surface paramagnetic relaxation sinks occur. The possibility that water may coordinate directly to paramagnetic relaxation centers, thus favoring an IS relaxation enhancement mechanism, as in the case of the most commonly used Gd-based contrast agents, seems to be of minor importance, its contribution to the observed relaxation dispersion profiles being small with respect to that arising from the OS mechanism. The dominating OS relaxivity is indeed favored by the bundling of BNNTs, which is known to occur in water, and by the presence of the glycol-chitosan coating. As a matter of fact, water can be trapped in the interstices present in the bundles with an increase of local viscosity that enhances OS relaxation. A similar situation has been described for apoferritin.<sup>38</sup> In addition, the coating layer may change the distance of closest approach of water protons to the paramagnetic species and may influence both the diffusion of water and the chemical exchange processes with the bulk, as pointed out by other authors.<sup>39–44</sup> In particular, for hydrophilic coating materials, such as glycol-chitosan, the translational diffusion rate of water is reduced with respect to the bulk and there is less proton exchange between the layer and the bulk.

The dominance of the translational contribution to the paramagnetic relaxation enhancement of water protons permits a characterization of the water translational diffusion in the local environment of the paramagnetic center.<sup>45–47</sup> Indeed, since the population of water molecules at the interface generally mixes by exchange with the total population of the observed molecules and the electron–nuclear dipolar interaction falls rapidly with distance from the paramagnetic center, the motions of the observed diffusing molecules relative to the surface localized paramagnet may be characterized in the immediate vicinity of the paramagnetic center. Following the theory developed by Korb et al.<sup>34,36</sup> the OS contribution to relaxivity can be written as

$$r_1^{\text{OS}} = \frac{1}{[\text{Gd}]} \frac{N_{\text{surf}}}{N} \frac{\pi}{30} \left( \frac{\mu_0}{4\pi} \right)^2 \gamma_{\text{H}}^2 g^2 \mu_{\text{B}}^2 S(S+1) \frac{\sigma_{\text{S}}}{\lambda^2 \delta^2} \times \tau_{\text{d}} \left[ 3 \ln \left( \frac{1 + \omega_{\text{H}}^2 \tau_{\text{d}}^2}{(\tau_{\text{d}}/\tau_{\text{s}})^2 + \omega_{\text{H}}^2 \tau_{\text{d}}^2} \right) + 7 \ln \left( \frac{1 + \omega_{\text{e}}^2 \tau_{\text{d}}^2}{(\tau_{\text{d}}/\tau_{\text{s}})^2 + \omega_{\text{e}}^2 \tau_{\text{d}}^2} \right) \right] \quad (4)$$

where:  $\gamma_{\text{H}}$  is the gyromagnetic ratio of proton ( $4.258 \times 10^6 \text{ s}^{-1} \text{ T}^{-1}$ );  $g$  is the Landé factor ( $g \cong 2$ );  $\mu_{\text{B}}$  is the Bohr magneton ( $9.274 \times 10^{-24} \text{ J T}^{-1}$ );  $S$  is the spin of the paramagnetic species ( $S = 7/2$  for Gd);  $N_{\text{surf}}/N$  is the ratio between the water molecules within the layer of thickness  $\lambda$  close to the surface, undergoing two-dimensional diffusion, and the water molecules in the bulk, and is hence proportional to  $\lambda$ ;  $\mu_0$  is the vacuum permeability ( $1.256 \times 10^{-6} \text{ N A}^{-2}$ );  $\omega_{\text{e}}$  and  $\omega_{\text{H}}$  are the electron and proton resonance frequencies (in  $\text{rad s}^{-1}$ ), respectively ( $\omega_{\text{e}} = 658 \omega_{\text{H}}$ );  $\sigma_{\text{S}}$  is the surface density of paramagnetic species;  $\delta$  is the distance of closest approach between water protons and paramagnetic species;  $\tau_{\text{d}}$  is the diffusion correlation time; and  $\tau_{\text{s}}$  is the residence time of water molecules in the surface layer (Figure 4). In order to quantitatively describe the diffusion and

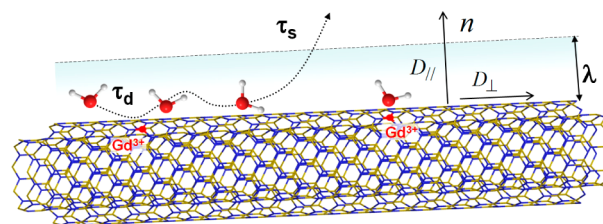


**Figure 4.** Schematic representation of the model used for the outer sphere relaxivity in BNNTs. The two-dimensional translational diffusion of the water molecules is described by an unbounded diffusion perpendicular to the axis normal to the nanotube surface ( $n$ ) and a bounded diffusion parallel to  $n$ .  $D_{||}$  and  $D_{\perp}$  are the translational diffusion coefficients in direction parallel and perpendicular to  $n$ , respectively. The diffusion correlation time is  $\tau_{\text{d}} = \delta^2/4D_{\perp}$ ,  $\delta$  being the distance of closest approach between water protons and paramagnetic species.  $\tau_{\text{s}}$  is the residence time of water molecules in the layer of thickness  $\lambda$ .

surface affinity properties of water, the Gd@BNNT  $r_1$  dispersion was fitted considering a constant term for  $r_1^{\text{IS}}$ , to avoid overinterpretation of the data, and eq 4 for  $r_1^{\text{OS}}$ , taking as fitting parameters  $\tau_{\text{d}}$ ,  $\tau_{\text{s}}$ ,  $r_1^{\text{IS}}$ , and a global constant  $K$  given by

$$K = \frac{N_{\text{surf}}}{N} \frac{\pi}{30} \left( \frac{\mu_0}{4\pi} \right)^2 \gamma_{\text{H}}^2 g^2 \mu_{\text{B}}^2 S(S+1) \frac{\sigma_{\text{S}}}{\lambda^2 \delta^2} \quad (5)$$

A nonlinear least-squares fitting was performed on the  $r_1$  data collected at 28, 37, and 46 °C; as shown in Figure 3, a good reproduction was obtained in all cases with the best fit parameters reported in Table 1. The  $r_1^{\text{IS}}$  values, which are practically equal at all temperatures, are comparable to those generally found for macromolecular and nanosized Gd-based contrast agents.<sup>12,48</sup> Unfortunately, the lack of clear features characteristic of the IS relaxivity prevents here a detailed analysis of the parameters governing this mechanism. The data only allowed the relative contribution of  $r_1^{\text{IS}}$  to the overall relaxivity to be estimated at the different Larmor frequencies, this becoming predominant only above 10 MHz (see Figure S3 in Supporting Information).

**Table 1.** Best Fit Parameters Obtained from the Analysis of the  $r_1$  NMRD Curves of Gd@BNNTs Reported in Figure 3

$T$ (°C)	$r_1^{\text{IS}}$ (mM $^{-1}$ s $^{-1}$ )	$K$ (s $^{-2}$ )	$\tau_d$ (s)	$\tau_s$ (s)
28	$8.4 \pm 0.9$	$(1.8 \pm 0.2) 10^6$	$(2.7 \pm 0.3) 10^{-8}$	$(10 \pm 2) 10^{-6}$
37	$8.5 \pm 0.9$	$(2.4 \pm 0.2) 10^6$	$(2.1 \pm 0.2) 10^{-8}$	$(8 \pm 2) 10^{-6}$
46	$8.5 \pm 0.9$	$(3.2 \pm 0.2) 10^6$	$(1.7 \pm 0.1) 10^{-8}$	$(6 \pm 1) 10^{-6}$

The best fit values of  $K$ ,  $\tau_s$ , and  $\tau_d$  parameters can be used to semiquantitatively characterize water behavior in the proximity of the nanotube surface. Considering that, according to the model,  $\tau_d = \delta^2/4D_L$ , the minimum value of the water translational diffusion coefficient in the surface layer, calculated considering the distance of closest approach  $\delta$  equal to the water radius (i.e., 0.3 nm), is  $(8 \pm 2) 10^{-13}$  m $^2$  s $^{-1}$ . This value is 3 orders of magnitude lower than that of free water and it is therefore indicative of a significant slowing down of the water molecule translational motion along the surface, in analogy to what observed for other contrast agents where water confinement is strongly involved in relaxation enhancement.<sup>38,41</sup> Both  $\tau_d$  and  $\tau_s$  show a decreasing trend with increasing the temperature. The  $\tau_s/\tau_d$  ratio, which corresponds to the number of molecular diffusing steps on the surface before escape from the surface layer and hence can be considered as a measure of the affinity of water for the nanotube surface, is  $\sim 370$  in all cases. This value indicates a high affinity of water for the surface at all the temperatures. The parameter  $K$  increases with increasing the temperature (Table 1). This finding can be essentially accounted for with a decrease of  $\lambda$ , the thickness of the layer of water undergoing restricted two-dimensional diffusion on the nanotube surface.  $\lambda$  values ranging from 1.4 to 2.6 nm, on going from 46 to 28 °C, are obtained from  $K$  using eq 5 with the same  $\delta$  value given above and values of  $\sigma_s$  ( $\cong 10^{17}$  Gd m $^{-2}$ ) and  $N_{\text{surf}}/N\lambda$  ( $\cong 10^4$  m $^{-1}$ ) estimated on the basis of known properties of the Gd@BNNTs investigated.<sup>25</sup> The trend of  $\lambda$  with temperature can be ascribed to a decrease of the population of the water molecules undergoing restricted two-dimensional diffusion with increasing the temperature, as discussed by Godefroy et al.<sup>27</sup>

The same model for relaxation enhancement could also be used to describe the  $R_1$  dispersions acquired for BNNTs with very good agreement between experimental data and calculated curves, obtaining  $\tau_d$  and  $\tau_s$  best fit values on the same order of those determined for Gd@BNNTs (see  $R_1$  dispersion analysis in the Supporting Information). These findings indicate that, irrespective of the paramagnetic species involved in water relaxation enhancement, the relaxation mechanism is dominated by the restricted diffusion of water on the nanotube surface.

## CONCLUSIONS

In this work,  $^1\text{H}$  longitudinal relaxivity has been investigated at low frequency (0.01–30 MHz) on Gd@BNNT water suspensions in order to unravel the mechanism of water proton relaxation at the basis of the potential application of Gd@BNNTs as contrast agents proposed in a previous work<sup>7</sup> on account of  $T_1$  and  $T_2$  relaxivity at high field (7 T) and biocompatibility properties.

The Gd@BNNT longitudinal relaxivity data acquired in the previous and in the present work may be used to better evaluate the potential efficacy of these systems as advanced MRI CAs. The remarkably high values of  $r_1$  at very low fields ( $\sim 0.01$

MHz) will especially be exploited in microtesla MRI imaging technologies.<sup>22,49</sup> At conventional magnetic fields (20–60 MHz), the longitudinal relaxivity of Gd@BNNTs is quite lower than that of clinically used Gd-based contrast agents, and becomes on the same order of magnitude at high field ( $3.5 \pm 0.5$  mM $^{-1}$  s $^{-1}$  at 7 T) where, on the other hand, transverse relaxivity is very high ( $380 \pm 30$  mM $^{-1}$  s $^{-1}$ ).<sup>7</sup>

Thanks to the sensitivity of the NMRD response to the solvation of the nanostructure, particularly at low frequency, it has been possible to get insight into the mechanism of water proton relaxation enhancement induced by Gd $^{3+}$  ions on the BNNT surface. The longitudinal relaxivity properties have been found to be mostly determined by an outer sphere mechanism at low frequencies and by an inner sphere mechanism at high frequencies. The features of the  $r_1$  NMRD curves did not allow an accurate analysis of the inner sphere contribution to be performed, whereas the outer sphere contribution could be analyzed in details in terms of restricted two-dimensional diffusion. By applying a suitable model, the dynamic properties of water in proximity of the nanotube surface could be quantitatively characterized. This information is difficult to obtain by other techniques and is of relevance for biomedical applications and for understanding assembling processes. In the case of BNNTs and other nanosized contrast agents requiring a coating to be suspended in water, the analysis of NMRD curves may allow information on the influence of the coating material on water diffusion in proximity of the nanostructure surface to be obtained. To this respect, investigations of NMR dispersions as a function of the coating chemico-physical properties and thickness would help in discerning the role played by the coating not only in cytotoxicity, solubility, aggregation, transport, and biodistribution properties,<sup>50</sup> but also in contrast properties.

## ASSOCIATED CONTENT

### Supporting Information

Trends of water proton  $R_1$  vs concentration measured for BNNT and Gd@BNNT suspensions at 37 °C; quantitative analysis of water proton  $R_1$  dispersions determined for BNNTs; inner sphere and outer sphere contributions to Gd@BNNT relaxivity at 37 °C as a function of Larmor frequency. This material is available free of charge via the Internet at <http://pubs.acs.org>.

## AUTHOR INFORMATION

### Corresponding Author

\*Phone: +39-050-3152517. Fax: +39-050-3152555. E-mail: [lucia.calucci@pi.iccom.cnr.it](mailto:lucia.calucci@pi.iccom.cnr.it).

### Author Contributions

The manuscript was written through contributions of all authors. All authors have given approval to the final version of the manuscript.

### Notes

The authors declare no competing financial interest.

## ACKNOWLEDGMENTS

M. C. Mascherpa is thanked for performing ICP-OES analysis. Beneficentia Stiftung is kindly acknowledged for financial contribution.

## ■ ABBREVIATIONS:

BNNT: boron nitride nanotube; CA: contrast agent; FFC: fast field-cycling; Gd@BNNT: Gd-doped boron nitride nanotube; IS: inner sphere; MRI: magnetic resonance imaging; NMRD: nuclear magnetic resonance dispersion; OS: outer sphere; PRE: paramagnetic relaxation enhancement

## ■ REFERENCES

- (1) Ciofani, G.; Raffa, V.; Mencias, A.; Cuschieri, A. Boron Nitride Nanotubes: an Innovative Tool for Nanomedicine. *Nano Today* **2009**, *4*, 8–10.
- (2) Terrones, M.; Romo-Herrera, J. M.; Cruz-Silva, E.; Lopez-Urias, F.; Munoz-Sandoval, E.; Velazquez-Salazar, J. J.; Terrones, H.; Bando, Y.; Golberg, D. Pure and Doped Boron Nitride Nanotubes. *Mater. Today* **2007**, *10*, 30–38.
- (3) Golberg, D.; Bando, Y.; Tang, C. C.; Zhi, C. Y. Boron Nitride Nanotubes. *Adv. Mater.* **2007**, *19*, 2413–2432.
- (4) Zhi, C.; Bando, Y.; Tang, C.; Golberg, D. Boron Nitride Nanotubes. *Mater. Sci. Eng. R* **2010**, *70*, 92–111.
- (5) Golberg, D.; Bando, Y.; Huang, Y.; Terao, T.; Mitome, M.; Tang, C.; Zhi, C. Boron Nitride Nanotubes and Nanosheets. *ACS Nano* **2010**, *4*, 2979–2993.
- (6) Ciofani, G.; Danti, S.; Genchi, G. G.; Mazzolai, B.; Mattoli, V. Boron Nitride Nanotubes: Biocompatibility and Potential Spill-Over in Nanomedicine. *Small* **2013**, *9*, 1672–1685.
- (7) Ciofani, G.; Boni, A.; Calucci, L.; Forte, C.; Gozzi, A.; Mazzolai, B.; Mattoli, V. Gd-Doped BNNTs as T<sub>2</sub>-Weighted MRI Contrast Agents. *Nanotechnology* **2013**, *24*, 315101.
- (8) Sitharaman, B.; Kissell, K. R.; Hartman, K. B.; Tran, L. A.; Baikalov, A.; Rusakova, I.; Sun, Y.; Khant, H. A.; Ludtke, S. J.; Chiu, W.; Laus, S.; Tóth, E.; Helm, L.; Merbach, A. E.; Wilson, L. J. Superparamagnetic Gadonanotubes Are High-Performance MRI Contrast Agents. *Chem. Commun.* **2005**, 3915–3917.
- (9) Sitharaman, B.; Wilson, L. J. Gadonanotubes as New High-Performance MRI Contrast Agents. *Int. J. Nanomed.* **2006**, *1*, 291–295.
- (10) Richard, C.; Doan, B.-T.; Beloeil, J.-C.; Bessodes, M.; Tóth, É.; Scherman, D. Noncovalent Functionalization of Carbon Nanotubes with Amphiphilic Gd<sup>3+</sup> Chelates: Toward Powerful T<sub>1</sub> and T<sub>2</sub> MRI Contrast Agents. *Nano Lett.* **2008**, *8*, 232–236.
- (11) Ananta, J. S.; Godin, B.; Sethi, R.; Moriggi, L.; Liu, X.; Serda, R. E.; Krishnamurthy, R.; Muthupillai, R.; Bolskar, R. D.; Helm, L.; Ferrari, M.; Wilson, L. J.; Decuzzi, P. Geometrical Confinement of Gadolinium-Based Contrast Agents in Nanoporous Particles Enhances T<sub>1</sub> Contrast. *Nat. Nanotechnol.* **2010**, *5*, 815–821.
- (12) Botta, M.; Tei, L. Relaxivity Enhancement in Macromolecular and Nanosized Gd<sup>III</sup>-Based MRI Contrast Agents. *Eur. J. Inorg. Chem.* **2012**, 1945–1960.
- (13) Meledandri, C. J.; Brougham, D. F. Low Field Magnetic Resonance Techniques in the Development of Nanomaterials for Biomedical Applications. *Anal. Methods* **2012**, *4*, 331–341.
- (14) Johnson, N. J. J.; Oakden, W.; Stanis, G.; Prosser, R. S.; van Veggel, F. C. J. M. Size-Tunable, Ultrasmall NaGdF<sub>4</sub> Nanoparticles: Insights into Their T<sub>1</sub> MRI Contrast Enhancement. *Chem. Mater.* **2011**, *23*, 3714–3722.
- (15) Paratala, B. S.; Jacobson, B. D.; Kanakia, S.; Francis, L. D.; Sitharaman, B. Physicochemical Characterization, and Relaxometry Studies of Micro-Graphite Oxide, Graphene Nanoplatelets, and Nanoribbons. *PLoS One* **2012**, *7*, e38185.
- (16) Sitharaman, B.; Jacobson, B. D.; Wadghiri, Y. Z.; Bryant, H.; Frank, J. The Magnetic, Relaxometric, and Optical Properties of Gadolinium-Catalyzed Single Walled Carbon Nanotubes. *J. Appl. Phys.* **2013**, *113*, 134308.
- (17) Hung, A. H.; Duch, M. C.; Parigi, G.; Rotz, M. W.; Manus, L. M.; Mastarone, D. J.; Dam, K. T.; Gits, C. C.; MacRenaris, K. W.; Luchinat, C.; Hersam, M. C.; Meade, T. J. Mechanisms of Gadographene-Mediated Proton Spin Relaxation. *J. Phys. Chem. C* **2013**, *117*, 16263–16273.
- (18) Chen, F.; Bu, W.; Zhang, S.; Liu, J.; Fan, W.; Zhou, L.; Peng, W.; Shi, J. Gd<sup>3+</sup>-Ion-Doped Upconversion Nanoprobes: Relaxivity Mechanism Probing and Sensitivity Optimization. *Adv. Funct. Mater.* **2013**, *23*, 298–307.
- (19) Carniato, F.; Tei, L.; Arrais, A.; Marchese, L.; Botta, M. Selective Anchoring of Gd<sup>III</sup> Chelates on the External Surface of Organo-Modified Mesoporous Silica Nanoparticles: A New Chemical Strategy to Enhance Relaxivity. *Chem.—Eur. J.* **2013**, *19*, 1421–1428.
- (20) Delli Castelli, D.; Gianolio, E.; Geninatti Crich, S.; Terreno, E.; Aime, S. Metal Containing Nanosized Systems for MR-Molecular Imaging Applications. *Coord. Chem. Rev.* **2008**, *252*, 2424–2443.
- (21) Terreno, E.; Delli Castelli, D.; Viale, A.; Aime, S. Challenges for Molecular Magnetic Resonance Imaging. *Chem. Rev.* **2010**, *110*, 3019–3042.
- (22) Davies, G.-L.; Corr, S. A.; Meledandri, C. J.; Briode, L.; Brougham, D. F.; Gun'ko, Y. K. NMR Relaxation of Water in Nanostructures: Analysis of Ferromagnetic Cobalt-Ferrite Polyelectrolyte Nanocomposites. *ChemPhysChem* **2011**, *12*, 772–776.
- (23) Berorizky, E. J.; Fries, P. H.; Guillermo, A.; Poncelet, O. Almost Ideal 1D Water Diffusion in Imogolite Nanotubes Evidenced by NMR Relaxometry. *ChemPhysChem* **2010**, *11*, 2021–2026.
- (24) Kimmich, R.; Anardo, E. Field-Cycling NMR Relaxometry. *Prog. Nucl. Magn. Reson. Spectrosc.* **2004**, *44*, 257–320.
- (25) Zhang, L.; Wang, J.; Gu, Y.; Zhao, G.; Qian, Q.; Li, J.; Pan, X.; Zhang, Z. Catalytic Growth of Bamboo-like Boron Nitride Nanotubes Using Self-Propagation High Temperature Synthesized Porous Precursor. *Mater. Lett.* **2012**, *67*, 17–20.
- (26) Korb, J.-P.; Whaley-Hodges, M.; Gobron, Th.; Bryant, R. G. Anomalous Surface Diffusion of Water Compared to Aprotic Liquids in Nanopores. *Phys. Rev. E* **1999**, *60*, 3097–3106.
- (27) Godefroy, S.; Korb, J.-P.; Fleury, N.; Bryant, R. G. Surface Nuclear Magnetic Relaxation and Dynamics of Water and Oil in Macroporous Media. *Phys. Rev. E* **2001**, *64*, 021605.
- (28) Lauffer, R. B. Paramagnetic Metal Complexes as Water Proton Relaxation Agents for NMR Imaging: Theory and Design. *Chem. Rev.* **1987**, *87*, 901–927.
- (29) Caravan, P.; Ellison, J. J.; McMurry, T. J.; Lauffer, R. B. Gadolinium(III) Chelates as MRI Contrast Agents: Structure, Dynamics, and Applications. *Chem. Rev.* **1999**, *99*, 2293–2352.
- (30) Helm, L. Relaxivity in Paramagnetic Systems: Theory and Mechanisms. *Prog. Nucl. Magn. Reson. Spectrosc.* **2006**, *49*, 45–64.
- (31) Kruk, D.; Kowalewski, J. General Treatment of Paramagnetic Relaxation Enhancement Associated with Translational Diffusion. *J. Chem. Phys.* **2009**, *130*, 174104.
- (32) Korb, J.-P.; Louis-Joseph, A.; Benamsili, L. Probing Structure and Dynamics of Bulk and Confined Crude Oils by Multiscale NMR Spectroscopy, Diffusometry, and Relaxometry. *J. Phys. Chem. B* **2013**, *117*, 7002–7014.
- (33) Victor, K. G.; Korb, J.-P.; Bryant, R. G. Translational Dynamics of Water at the Phospholipid Interface. *J. Phys. Chem. B* **2013**, *117*, 15475–15478.
- (34) Korb, J.-P.; Whaley-Hodges, M.; Bryant, R. G. Translational Diffusion of Liquids at Surfaces of Microporous Materials: Theoretical Analysis of Field-Cycling Magnetic Relaxation Measurements. *Phys. Rev. E* **1997**, *56*, 1934–1945.
- (35) Korb, J.-P.; Whaley-Hodges, M.; Bryant, R. G. Translational Diffusion of Liquids at Surface of Microporous Materials: New Theoretical Analysis of Field Cycling Magnetic Relaxation Measurements. *Magn. Reson. Imaging* **1998**, *16*, 575–578.
- (36) Korb, J.-P.; Freiman, G.; Nicot, B.; Ligneul, P. Dynamical Surface Affinity of Diphasic Liquids as a Probe of Wettability of Multimodal Porous Media. *Phys. Rev. E* **2009**, *80*, 061601.
- (37) Grebenkov, D. S.; Goddard, Y. A.; Diakova, G.; Korb, J.-P.; Bryant, R. G. Dimensionality of Diffusive Exploration at the Protein Interface in Solution. *J. Phys. Chem. B* **2009**, *113*, 13347–13356.
- (38) Fries, P. H.; Berorizky, E. J. Enhancement of the Water Proton Relaxivity by Trapping Gd<sup>3+</sup> Complexes in Nanovesicles. *J. Chem. Phys.* **2010**, *133*, 024504.



- (39) Duan, H.; Kuang, M.; Wang, X.; Wang, Y. A.; Mao, H.; Nie, S. Reexamining the Effects of Particle Size and Surface Chemistry on the Magnetic Properties of Iron Oxide Nanocrystals: New Insights into Spin Disorder and Proton Relaxivity. *J. Phys. Chem. C* **2008**, *22*, 8127–8131.
- (40) Daou, T. J.; Grenèche, J. M.; Pourroy, G.; Buathong, S.; Derory, D.; Ulhaq-Bouillet, C.; Donnio, B.; Guillon, D.; Begin-Colin, S. Coupling Agent Effect on Magnetic Properties of Functionalized Magnetite-Based Nanoparticles. *Chem. Mater.* **2008**, *20*, 5869–5875.
- (41) LaConte, L. E. W.; Nitin, N.; Zurkiya, O.; Caruntu, D.; O'Connor, C. J.; Hu, X.; Bao, G. Coating Thickness of Magnetic Iron Oxide Nanoparticles Affects  $R_2$  Relaxivity. *J. Magn. Reson. Imaging* **2007**, *26*, 1634–1641.
- (42) de Haan, H. W.; Paquet, C. Enhancement and Degradation of the  $R_2^*$  Relaxation Rate Resulting From the Encapsulation of Magnetic Particles with Hydrophilic Coating. *Magn. Reson. Med.* **2011**, *66*, 1759–1766.
- (43) Pinho, S. L. C.; Pereira, G. A.; Voisin, P.; Kassem, J.; Bouchaud, V.; Etienne, L.; Peters, J. A.; Carlos, L.; Mornet, S.; Galdes, C. F. G. C.; Rocha, J.; Delville, M.-H. Fine Tuning of the Relaxometry of  $\gamma$ - $\text{Fe}_2\text{O}_3/\text{SiO}_2$  Nanoparticles by Tweaking the Silica Coating Thickness. *ACS Nano* **2010**, *4*, 5339–5349.
- (44) Hong, T.; Lazarenko, R. M.; Colvin, D. C.; Flores, R. L.; Zhang, Q.; Xu, Y.-Q. Effect of Competitive Surface Functionalization and Magnetic Resonance Imaging of Single-Walled Carbon Nanotubes. *J. Phys. Chem. C* **2012**, *116*, 16318–16324.
- (45) Korb, J.-P.; Winterhalter, M.; McConnell, H. M. Theory of Spin Relaxation by Translational Diffusion in Two-Dimensional Systems. *J. Chem. Phys.* **1984**, *80*, 1059–1067.
- (46) Polnaszek, C. F.; Bryant, R. G. Nitroxide Radical Induced Solvent Proton Relaxation: Measurement of Localized Translational Diffusion. *J. Chem. Phys.* **1984**, *81*, 4038–4045.
- (47) Diakova, G.; Goddard, Y.; Korb, J.-P.; Bryant, R. G. Water-Proton-Spin-Lattice-Relaxation Dispersion of Paramagnetic Protein Solutions. *J. Magn. Reson.* **2011**, *208*, 195–203.
- (48) Rohrer, M.; Bauer, H.; Mintorovitch, J.; Requardt, M.; Weinmann, H.-J. Comparison of Magnetic Properties of MRI Contrast Media Solutions at Different Magnetic Field Strengths. *Invest. Radiol.* **2005**, *40*, 715–724.
- (49) Trahms, L.; Burghoff, M. NMR at Very Low Fields. *Magn. Reson. Imaging* **2010**, *28*, 1244–1250.
- (50) Issa, B.; Qadri, S.; Obaidat, I. M.; Bowtell, R. W.; Haik, Y. PEG Coating Reduces NMR Relaxivity of  $\text{Mn}_{0.5}\text{Zn}_{0.5}\text{Gd}_{0.02}\text{Fe}_{1.98}\text{O}_4$  Hyperthermia Nanoparticles. *J. Magn. Reson. Imaging* **2011**, *34*, 1192–1198.